Tight-binding theory for the thermal evolution of optical band gaps in semiconductors and superlattices

S. Abdollahi Pour, B. Movaghar, and M. Razeghi

Center for Quantum Devices, Electrical Engineering and Computer Science, Northwestern University, Evanston, Illinois 60208, USA

(Received 13 December 2010; revised manuscript received 21 January 2011; published 28 March 2011)

A method to handle the variation of the band gap with temperature in direct band-gap III–V semiconductors and superlattices using an empirical tight-binding method has been developed. The approach follows closely established procedures and allows parameter variations which give rise to perfect fits to the experimental data. We also apply the tight-binding method to the far more complex problem of band structures in type-II infrared superlattices for which we have access to original experimental data recently acquired by our group. Given the close packing of bands in small band-gap type-II designs, $\vec{k}\cdot\vec{p}$ methods become difficult to handle, and it turns out that the sp^3s^* tight-binding scheme is a practical and powerful asset. Other approaches to band-gap shrinkage explored in the past are discussed, scrutinized, and compared. This includes the lattice expansion term, the phonon softening mechanism, and the electron-phonon polaronic shifts calculated in perturbation theory.

DOI: 10.1103/PhysRevB.83.115331 PACS number(s): 78.55.Cr, 71.20.−b, 42.25.Bs, 71.38.−k

I. INTRODUCTION

Understanding the change in the band gap as a function of temperature in semiconductors has been a subject of great interest to the solid-state community for many years. All previous studies in this area can be divided into two main categories: empirical efforts to provide a universal fit that can be applied to a wide range of semiconductors[1,2] and efforts to explain the band-gap shrinkage using band-structure models based on the thermal expansion of the solid and the electron-phonon interactions.[3–6]

On the empirical front, the most famous work is by Varshni,[1] whose equation is widely used in the semiconductor community. However, the Varshni equation tends to overestimate the band-gap shrinkage at low temperatures and provides no physical insight into the phenomena.

Much work has been devoted to finding an empirical equation that has the generality of the Varshni equation, and is more accurate. Most of the recent work in this area has been done by Pässler.[2] His two-oscilator model provides an almost perfect fit to the experimental data, but it has an additional fitting variable. The underlying assumption in his work is the following standard thermodynamic rule based on the quasiharmonic approximation:

$$\frac{1}{\kappa}\frac{\Delta V}{V}=\sum_{\bar{q}}\gamma\hbar\omega_{\bar{q}}\frac{1}{2}\coth\left(\frac{\hbar\omega_{\bar{q}}}{2kT}\right), \tag{1}$$

which links volume expansion to thermal energy, where κ is the compressibility and γ is the Grüneisen constant. The volume expansion is then linked to the band gap via, for example, the Kane band-structure theory.[7] Although this fitting procedure is apparently closely related to the actual physical processes that are causing the change via Eq. (1), and despite an extensive numerical analysis,[8] it actually reveals very little about the mechanisms, except that they are obviously related to the phonon spectra. O'Donnell *et al.*[9] had gone even further and obtained some reasonable fits with only one phonon mode.

Aside from the empirical efforts, when looking at the overall explanations offered in the literature for band-gap shrinkage with temperature, they can be divided into two parts. One mechanism invoked is the thermal expansion and the other mechanism is thought to be due to the electron-phonon interaction. Since most of the first-principles methods for deriving the gap change rely on the perturbation methods, in which the ion-ion potential is treated in the harmonic potential approximation, they cannot directly take into account the anharmonicity term which causes the absolute expansion. Consequently, the change caused by the expansion of the lattice is treated through other methods. One method is to relate the change in temperature to change in pressure and deduce the thermal expansion term:[6,9]

$$\left[\frac{\partial E_g}{\partial T}\right]_{\text{thermal exp}}=-3B\alpha\left[\frac{\partial E_g}{\partial P}\right]_V, \tag{2}$$

where B is the bulk modulus, α is the thermal expansion coefficient, and P is pressure. Equation (2) is directly related to the thermodynamic relation in Eq. (1), on which the Pässler and O'Donnell theories are based. It is argued that the average expansion effect by itself is not enough[10] and the effect of the electron-phonon coupling on the energy levels has to be treated explicitly. The energy renormalization, produced by the electron-phonon interaction, is normally divided into two terms: The first-order change of the potential with lattice displacement is usually treated in second-order perturbation. This is known in the literature as the Fan[3] or polaronic self-energy term. The second-order change in the potential caused by displacements is taken into account using first-order perturbation. This is the so-called Debye-Waller (DW) term.[5,6] There is another mechanism first proposed by Heine *et al.*[11] and then developed further by Ridley[12] that assumes the band-gap change is due to the free-energy change caused by the softening of the phonon modes in response to the presence of electron-hole pairs. This mechanism was examined but was ruled out as an influential mechanism.

In the present investigation, we have analyzed these physical mechanisms and have identified the main reasons that cause the band-gap change with temperature in this particular class of III–V semiconductors. We start by introducing a method for calculating the shrinkage of the band gap with temperature using the empirical tight-binding (TB) method. The expansion of the lattice and the dynamical DW effects are assumed to change the overlap interaction energy of the TB orbitals.

The polaronic self-energy is also calculated, but is shown to give a relatively small contribution. The TB band-structure method has also been applied to the far more complex problem of the type-II InAs/GaSb superlattice (SL). In Sec. II, the theory will be developed. In Sec. III the comparison between theory and experiment is drawn, and Sec. IV introduces photoluminescence data for type-II SL and the developed theory will be applied to this more complex material system.

II. THEORY OF BAND-GAP SHRINKAGE WITH TEMPERATURE

A. Average and dynamical structural change

We first start by calculating the effect of the lattice expansion with temperature. The TB language provides a direct and natural way of expressing the energy gap as a function of orbital energies and overlap parameters. From the work of Wei,[13] which uses the sp^3s^* method, we have been able to deduce an analytical relation between the $k=0$ direct band gap and the TB parameters for III–V materials, given by

$$2E_g = (E_{sa} - E_{pa}) + (E_{sc} - E_{pc}) + \{[(E_{sa} - E_{sc})^2 + 4(E_{sasc})^2]^{1/2} + [(E_{pa} - E_{pc})^2 + 4(E_{xaxc})^2]^{1/2}\}, \tag{3}$$

where a and c stand for anion and cation, E_{sa} and E_{pa} are the orbital energies in the Hamiltonian for s and p orbitals, respectively, E_{sasc} is the interaction term between s orbitals, and E_{xaxc} is the interaction term between p_x orbitals. Note that the overlap with s^* does not enter the formula for the direct band gap. The analytical derivation of band gaps and effective masses is one of the advantages of the TB method.[13]

The lattice expansion mainly affects the overlap of the orbitals. We use the d^{-n} scaling rule of overlaps:

$$E_{\alpha,\beta} = \frac{E^0_{\alpha,\beta}\left|\vec{R}^0_{ij}\right|^n}{\left(\left|\vec{R}^0_{ij} + \delta\vec{R}_{ij}(t)\right|\right)^n}, \tag{4}$$

where $\vec{R}^0_{ij}$ represents the equilibrium bond length at $T=0$ K and $\delta\vec{R}_{ij}(t)$ is the displacement at time t. The interaction energies at $T=77$ K are known from empirical fits to the band structure.[14] Different scaling rules for the interaction energy in the TB model have been proposed in the literature. While some suggest a d^{-2} universal scaling rule for all orbitals,[15,16] others have differentiated between different orbitals and used different scaling factors for each interaction term.[17–19] Here, for simplicity, we do not differentiate between different orbital-type–orbital-type interaction terms, and we assume all the orbitals follow the same scaling rule. However, we recognize that the choice of n, given the variations used by various authors, is truly motivated by empirical rules rather than fundamental first-principles ones. So we carry on with the same logic and discover that, with $n=2$, the change of the band gap is underestimated and correspondingly n is altered to fit the experimental data, allowing a reasonable and tolerable variation. This will be explored further in Sec. III, where we compare our theory to the experimental data.

Equation (4) can be used to calculate the interactions at any given temperature and time, knowing $\delta\vec{R}_{ij}(t)$. Since the electron and holes move much faster and have lattice vibrations, they can be assumed to be moving in a frozen thermally disordered lattice that is mapped onto a Bloch lattice with effective lattice constants. Once we have identified the effective thermally induced structure, we can then use the full power of the TB method to solve for the band structure. This will turn out to be of particularly great value for SLs, where other methods of dealing with thermal effects will face far more complicated scenarios. In order to define the lattice we can now proceed in two different ways:

(a) Consider the displacement-dependent overlap $E_{\alpha,\beta}[\delta\vec{R}_{ij}(t)]$, expand for the lattice displacements $[\delta\vec{R}_{ij}(t)]$ to second order, then take the time average of the overlap and treat these average overlaps as the effective overlaps appropriate for the thermal Bloch lattice.

(b) First calculate the mean-squared distance $\langle|\vec{R}^0_{ij} + \delta\vec{R}_{ij}(t)|^2\rangle$, and then define the root of the mean-squared distance as the lattice constant defining the effective Bloch lattice entering the denominator of Eq. (4).

The results of calculating the mean-squared values for interactions using scenarios (a) and (b) are shown in Eqs. (5a) and (5b), respectively:

$$\left\langle \frac{\left|\vec{R}^0_{ij}\right|^2}{\left(\left|\vec{R}^0_{ij} + \delta\vec{R}_{ij}(t)\right|\right)^2} \right\rangle = 1 - 2\frac{\langle|\delta\vec{R}_{ij}|\rangle}{\left|\vec{R}^0_{ij}\right|} + 3\frac{\langle|\delta\vec{R}_{ij}|^2\rangle}{\left|\vec{R}^0_{ij}\right|^2}, \tag{5a}$$

$$\frac{\left|\vec{R}^0_{ij}\right|^2}{\left\langle\left(\left|\vec{R}^0_{ij} + \delta\vec{R}_{ij}(t)\right|\right)^2\right\rangle} = 1 - 2\frac{\langle|\delta\vec{R}_{ij}|\rangle}{\left|\vec{R}^0_{ij}\right|} - \frac{\langle|\delta\vec{R}_{ij}|^2\rangle}{\left|\delta\vec{R}^0_{ij}\right|^2}. \tag{5b}$$

Both methods (a) and (b) are to some extent arbitrary and subject to empirical verification of results. Method (a) weighs the increase in overlap more than the decrease when two atoms approach each other as a result of thermal fluctuations, which consequently results in a second-order enhancement of the orbital overlaps due to the lattice vibrations, while method (b) first averages the displacements and favors the decrease of the average overlap both in first and second order. Adopting method (b) and using a Taylor expansion in Eq. (4), the band gap is evaluated using the overlaps now given by the following correction:

$$\Delta E_{\alpha,\beta} = -E^0_{\alpha,\beta}\left[n\frac{\langle|\delta\vec{R}_{ij}|\rangle}{R_{ij}} + \left(\frac{n(n-1)}{2}\frac{\langle|\delta\vec{R}_{ij}|^2\rangle}{\vec{R}^2_{ij}}\right)\right]. \tag{6}$$

The first term in Eq. (6) is due to the asymmetric interion forces favoring the larger displacements at large amplitude, and is described by the expansion coefficient of the lattice. $|\delta\vec{R}_{ij}(t)|$ is determined using the experimental values for the thermal expansion coefficient of the crystal. The second term, which is the mean squared of displacement, is the DW term, which can be treated in the harmonic limit. The reader should note that if we use method (a), i.e., if we expand Eq. (4) before carrying out the averaging, the significant second-order term in Eq. (6) will have an opposite sign, as shown in Eq. (5a), which increases the overlap. This means that the DW term in method (a) expands the band gap as we increase the temperature, which is in contradiction to the observations and usual conclusions in the literature. The same result is obtained if we use the perturbation theory to calculate the DW energy.

The first term in Eq. (6) is related to the average lattice expansion and will be calculated using the data banks for

thermal expansion coefficients. Using the Debye approximation and integrating over three branches, $\langle|\delta\vec{R}_{ij}|^2\rangle$ in the second term is calculated as follows:[20]

$$\langle|\delta\vec{R}_{i,j}|^2\rangle = 2\frac{9\hbar^2}{Mk_b\theta_D^3}T^2\int_0^{\theta/T}\left(\frac{1}{e^z-1}+\frac{1}{2}\right)z\,dz, \tag{7}$$

where θ_D is the Debye temperature, and M is the average ion mass and is calculated as follows:

$$\frac{2}{M} = \frac{1}{M_1}+\frac{1}{M_2}. \tag{8}$$

The factor of 2 in Eq. (7) comes from the fact that $\langle|\delta\vec{R}_{i,j}|^2\rangle = 2\langle|u_i^2|\rangle$, assuming that there is no time correlation between the vibration of atoms in sites i and j, which is a justified assumption given the very large number of phonon modes being excited at any finite temperature. We can now use Eq. (3) and expand it with respect to the interaction energies to determine the change in the band gap:

$$\Delta E_g \sim -\frac{2E_{sasc}\Delta E_{sasc}}{\left[(E_{sa}-E_{sc})^2+4E_{sasc}^2\right]^{1/2}} - \frac{2E_{xaxc}\Delta E_{xasc}}{\left[(E_{pa}-E_{pc})^2+4E_{xaxc}^2\right]^{1/2}}. \tag{9}$$

As can be seen, the change in the band gap is linearly dependent on the change in the interaction energies. This ensures a nearly linear behavior with respect to temperature at high temperatures, since the expansion coefficient is almost constant at high temperatures, and Eq. (7) becomes linear as well. At low temperature, however, both the temperature dependence of the expansion coefficient and Eq. (7) result in a strong nonlinearity of the change in the band gap. In most III–V materials the expansion term is actually negative at low T, so it turns out that it is the DW term that gives rise to the observed shrinkage in this limit. This model also directly justifies the assumption made by Cody *et al.* in Ref. 21 to linearly relate the band gap to the mean-squared lattice displacements in amorphous Si. The work of Cody *et al.* provides additional and strong justification for using Eq. (5b), and concluding that thermal disorder effectively "lowers (raises)" the band edges, albeit this time in a Bloch framework, not Urbach tails.

B. Electron (hole)-phonon interaction

Having defined the thermal Bloch lattice, we still have to allow the electrons and holes in this effective structure to interact with phonons and create polaronic distortions. This means, in effect, computing the polaron self-energy terms and neglecting the shifts in the phonon spectra caused by the thermal expansions. To obtain the polaron self-energy shift, it is more convenient to use the Hamiltonian in the Bloch representation assuming the $\varepsilon(\boldsymbol{k})$ dispersions and effective masses m_e^* and m_h^* generated by the TB method.[16,22] The Hamiltonian of the system, including the electron-phonon interaction, is as follows:

$$H = \sum_{k,\sigma}\varepsilon_{k,\sigma}c_{k,\sigma}^+c_{k,\sigma} + \sum_{\vec{k},\vec{q}}[C(\vec{q})e^{i\vec{q}\cdot\vec{r}}a_{\vec{q}}c_{k+q,\sigma}^+c_{k,\sigma} + \text{c.c.}], \tag{10}$$

where σ is the spin variable and $C(\vec{q})$ is the electron-phonon coupling. The coupling constant depends on the way one describes the energy bands, and in TB it is contained in Eq. (6). Here we choose the more general form given by Eq. (10) applied in the nearly free-electron limit. In this way we can use the standard and well-documented parametrization of the couplings from the literature. Thus the standard perturbation theory is used to calculate the polaron self-energy shift. The DW effect in our method is already accounted for in the definition of this unique lattice. Assuming parabolic energy bands for electrons and holes, Eqs. (11a) and (11b) describe the interaction of electrons (or holes) with phonons through emission and absorption to the first order, respectively:

$$\Delta E_{\text{emiss}}(s,\vec{k}) = \sum_{\vec{q}}|\langle\vec{k}|C_{\vec{q}}e^{-iqr}|\vec{k}-\vec{q}\rangle|^2 \times\frac{1+n(\omega_q)}{\left[\left(\frac{\hbar^2}{2m^*}(k^2-|\vec{k}-\vec{q}|^2)\right)-\hbar\omega_q\right]}, \tag{11a}$$

$$\Delta E_{\text{abs}}(s,\vec{k}) = \sum_{\vec{q}}|\langle\vec{k}|C_{\vec{q}}e^{-iqr}|\vec{k}-\vec{q}\rangle|^2 \times\frac{n(\omega_q)}{\left[\left(\frac{\hbar^2}{2m^*}(k^2-|\vec{k}-\vec{q}|^2)\right)-\hbar\omega_q\right]}, \tag{11b}$$

where s represents the energy band (valence or conduction band), $C(\vec{q})$ is the electron (hole)-phonon coupling, $\vec{k}$ and $\vec{q}$ are the electron and phonon wave numbers, respectively, ω_q is the phonon frequency, and m^* is the effective mass of the corresponding band.

The interaction of phonons with carriers can be divided into a number of main categories: LA phonons that contribute to dilation as well as shear deformation potential effects, TA phonons that contribute to the shear deformation potential effect, and piezoelectric phonons and LO phonons causing the so-called Fröhlich interaction.[4,23] It is known that for zinc-blende III–VI semiconductors, the main contributions are due to the dilation of the lattice as well as the Fröhlich term.

Using the deformation potential to estimate the effects of lattice dilation caused by the propagation of the phonons in the lattice, and estimating the dispersion of the phonons with the Debye approximation in Eqs. (11a) and (11b), respectively, we have the following expressions:

$$\Delta E_{\text{emiss}}^{\text{deform}}(s,k=0) = -\frac{1}{2\pi^2}(kT/\hbar\bar{v}_s)^3\frac{D^2}{2\rho v_s^2}\int_0^{\theta/T}dx\,x^2 \times\left(\frac{1}{e^x-1}\right)\frac{1}{\left(1+kTx/2v_s^2m^*\right)}, \tag{12a}$$

$$\Delta E_{\text{abs}}^{\text{deform}}(s,k=0) = -\frac{1}{2\pi^2}(kT/\hbar\bar{v}_s)^3\frac{D^2}{2\rho v_s^2}\int_0^{\theta/T}dx\,x^2 \times\left(\frac{1}{e^x-1}\right)\frac{1}{\left(1+kTx/2v_s^2m^*\right)}, \tag{12b}$$

which describe emission and absorption, respectively. The interaction term is assumed to be defined as

$$|\langle k|C_{\vec{q}}e^{-iqr}|k-q\rangle|^2 = \frac{1}{V}\frac{D^2}{2\rho v_s^2}\hbar\omega_{\vec{q}}, \tag{13}$$

where V is the volume, D is deformation potential, ρ is the density, and v_s is the sound velocity. In Eq. (12a), terms that are not temperature dependent were discarded. To estimate the significance of this interaction term, it is calculated at $T = 300$ K for GaAs. The values for the deformation potential vary for different phonon modes and, specifically, the experimental values cannot be easily measured for shear deformation potentials. Nonetheless, based on the values reported in the literature, it is recognized that typically $D < 10$ eV. Here the value of $D = 10$ eV is chosen to calculate the upper limit for this effect. This assumption results in $\Delta E = -13$ meV for GaAs at 300 K, if the effective mass is equal to the free-electron mass and the slowest velocity of sound of the three branches is chosen. Given that the total shift in the band gap from 0 from 300 K in GaAs is 93 meV,[24] the contribution from this term can be important or negligible depending on the value of the effective mass. The effective mass for electron is $m_e^* = 0.06m_0$, which results in <1 meV change in the band gap and is negligible. In the valence band, however, there are three different bands, and the effective masses range from $0.08m_0$ for light holes to $0.51m_0$ for heavy holes. The choice of effective mass can result in an order of magnitude change in the calculated energy shift. To find the relevant effective mass, we first recognize that all the band-gap data used in this paper and most of the data available in the literature are measured using optical methods (mainly photoluminescence or absorption). Consequently, the relevant valence band in Eqs. (12a) and (16b) should be the one that has the strongest momentum matrix element with the conduction band. Using the four-band Kane theory and applying the sum rule for the oscillator strength results in the following relation between the oscillator strength and effective masses:[12]

$$\sum_{m\neq n} f_{mn} = 1 - \frac{m}{m_n^*}, \tag{14}$$

where the indices m and n can be hh, lh, so, and c standing for heavy hole, light hole, spin orbit and conduction band, respectively. f is the oscillator strength. Assuming that the matrix element between two valence bands is negligible, the following can be concluded:[12]

$$f_{cv} = 1 + \frac{m}{m_v^*}, \tag{15}$$

where v can be any of the three valence bands. Considering the values of light-hole and heavy-hole effective masses in GaAs, it can be seen that the oscillator strength between the light holes and electrons is $\sim$6 times stronger than the heavy holes and the electrons. This ratio is $\sim$2.5 for the spin-orbit band, but the spin-orbit band is not important in determining the band gap. Therefore, the relevant effective mass to be used in Eqs. (12a) and (12b) is the light-hole effective mass. This conclusion can be justified intuitively as well. Since the effective mass is a measure of delocalization of the wave function, electrons and light holes are both highly mixed by the Kane matrix element and have a strong dipole overlap, while heavy holes are strongly localized and their dipole overlap with electrons is expected to be much smaller. Using the light-hole effective mass, the resulting energy shift for holes is also $\sim$1 meV and is negligible.

For optical phonons, the change in energy is as follows:[25]

$$\Delta E_e(T) \sim -2n(\omega_L)(\alpha_e + \alpha_{\rm lh})\hbar\omega_L, \tag{16}$$

where $\alpha_{e,\rm lh}$ are the Fröhlich constants for electrons and light holes and $n(\omega)$ is the Bose-Einstein distribution function. To estimate the significance of this effect, GaAs is considered again. $\alpha_e \sim 0.085$ for GaAs (Ref. 26) and can be calculated to be $\alpha_{\rm lh} = 0.1$ for light holes. The longitudinal optical phonon energy is $\sim$36 meV and Eq. (16) results in a ~ -4.4 meV change in band gap from 0 to 300 K, which is less than 5% of the total band-gap change over this temperature range in GaAs. The same arguments that were made for GaAs holds for other III–V compounds as well, and the polaron self-energy contribution to the band-gap shrinkage seems to be negligible in these materials. As a result, these terms are neglected in the data fitting.

However, it should be mentioned that the polaron shift can get much bigger if the carriers are in excitonic states when they recombine or even more so in localized trap levels. Anderson showed that localization considerably enhances the polaron self-interaction.[27] However, the focus of this work is on the band-edge shifts, and the data extracted refers, where possible, to energy shift corrected for excitonic effects. Therefore, in this paper, we are not considering an Anderson type of self-localization.

Cardona *et al.*[28] have measured the very low-temperature gap shift and have shown that it scales as T^4. This observation is justified using the electron-phonon interaction in Eq. (12) by assuming that coupling D vanishes for very long-wavelength phonons. It is recognized that this effect might create a small correction at very low temperatures, but defining the fine details of band-gap shrinkage at very low temperatures is not within the scope of the present work; rather, it is focused on finding the dominant mechanisms over the whole temperature range of 0–300 K. So, neglecting this effect in fitting the data does not introduce any error within the level of accuracy that we are trying to achieve.

III. FITTING THE THEORETICAL VALUES TO EXPERIMENTAL DATA FOR BULK MATERIAL

As we have discussed above, we conclude that the only substantial effects in determining the shrinkage of the band gap are the thermal expansion of the lattice and the DW broadening of the band edges in the framework of the effective lattice model with an order parameter $\langle|\vec{R}_{ij}|\rangle$. The other effects, polaron self-energy and phonon softening, account for less than 10% of the total shrinkage. In the data fitting of crystalline III–V materials, those effects will not be used. They are not needed to achieve a good fit, and their contribution is small. The objective here is to find the main mechanisms which can be used to explain and predict the thermal band-gap trends in SLs, especially in long and very long wavelengths in type-II

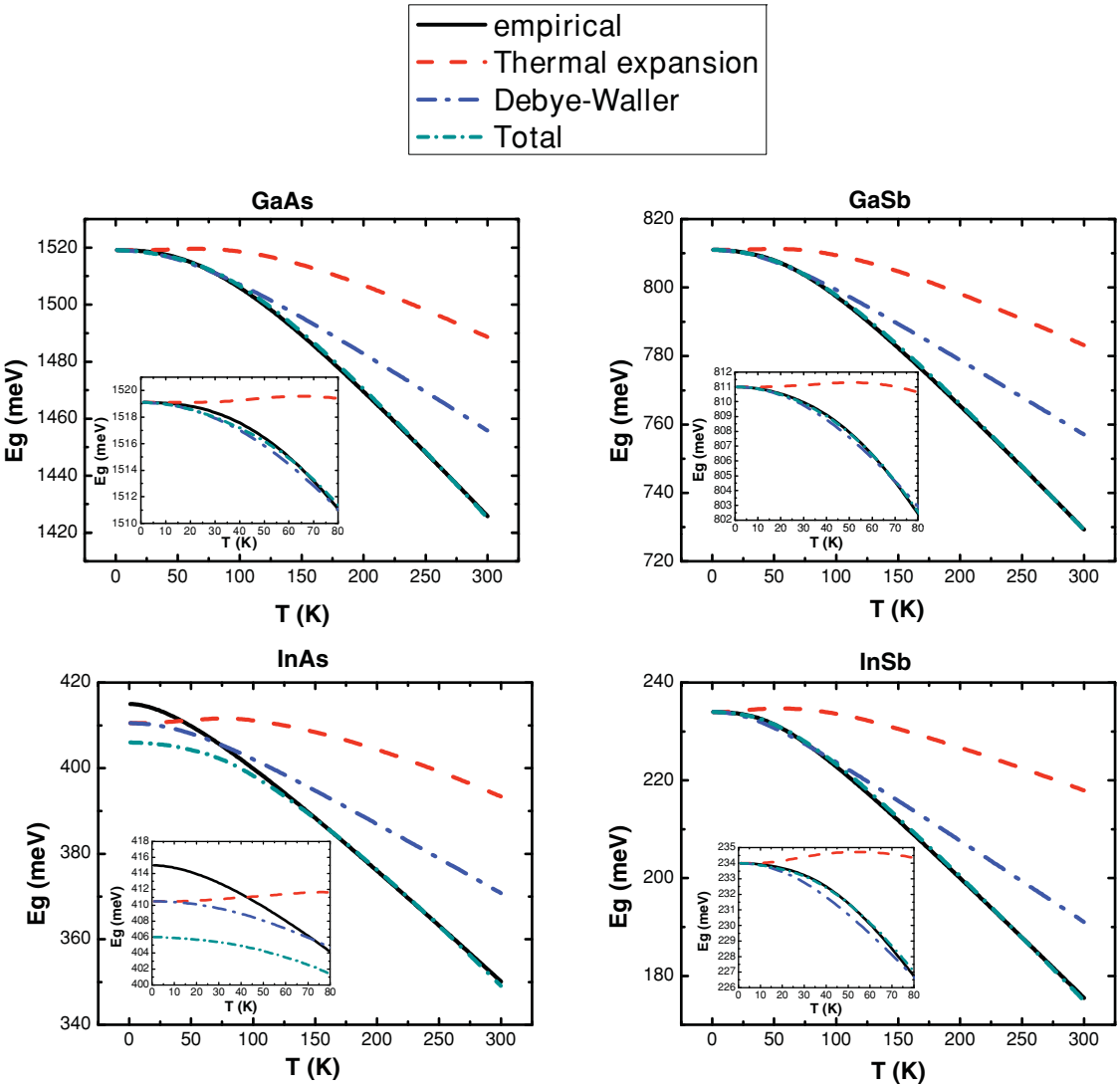

FIG. 1. (Color online) Comparison between theory and experiment for (a) GaAs, (b) GaSb, (c) InAs, and (d) InSb. The insets magnify the region between 0 and 80 K.

SLs, where the optical measurement of the band gap cannot be performed easily. As we shall see, this objective can be achieved by only considering thermal expansion and DW terms.

Figure 1 shows the result of the fitting to the experimental data for GaAs,[24] GaSb,[29] InAs,[30] and InSb.[30] These materials were chosen because they form the antimony-based type-II SL that is investigated in the next section. Pässler's two-oscillator fit was used as the empirical fit to the theory[31] since it almost gives a perfect fit to the experimental data. The interaction energies for the empirical TB method were taken from Vogl.[16] The thermal expansion coefficient and Debye temperatures were mainly taken from Ref. 32. The only fitting parameter used was n in Eq. (6).

In each case, the contribution is broken down into two components: the shrinkage caused by thermal expansion and the shrinkage caused by the DW term. Each component is plotted separately for the comparison. Since Eq. (9) gives a linear relation to overlap change, the total shrinkage is the sum of these two components. The thermal shift of the spin-orbit energy was neglected in these calculations. Table I shows the values of n chosen for each material. As can be seen, the theory predicts a nearly linear dependence of the band gap with temperature at high temperatures. The percentage of contribution of each component at high temperature is also listed in Table I. For all the materials the contribution from the lattice expansion is ∼40% of the total effect while the DW term is responsible for ∼60% of the change. This

TABLE I. Values of n in Eq. (6) that are chosen to fit the experimental data in different materials. The relative weight of thermal expansion and DW in the total band-gap shrinkage at linear regime (high temperature, 200–300 K) is also given.

Material	n	Expansion ratio (%)	Debye-Waller ratio (%)
GaAs	3.7	41	59
GaSb	3.3	40	60
InAs	2.9	42	58
InSb	2.95	38	62

empirical observation is interesting considering the fact that the value of n changes significantly from one material to the other. At low temperatures, the expansion coefficient of most III–V semiconductors is first negative and then turns positive as we go up beyond $T \sim 50$ K. The band gap, however, always shrinks with T even at very low T. Our theory provides a natural explanation of this effect. At low temperature, all the materials produce a perfect fit to the experiment except for InAs, where the experiment deviates ~9 meV from the theory at low temperatures. This discrepancy is most likely related to the experimental data available for InAs. This data show an unusually strong dependence of the band gap with temperature at low temperatures. InAs has a Debye temperature and expansion coefficient that is very close to GaSb, and the band gap is expected to behave in a similar qualitative form, but it behaves quite differently. However, a more reliable set of data for InAs could not be found in literature and the best fit to the existing data was utilized. The value of n ranges from 2.9 for InAs to 3.7 for GaAs.

IV. APPLYING THE THEORY TO TYPE-II InAs/GaSb SUPERLATTICE

The theory that was developed for the bulk material was applied to the type-II SL to explain the shrinkage of the band gap with temperature in this complex material system. We remind the reader that the type-II SL is a very special SL for which the band gap can be tuned to allow electron-hole photoexcitations and thus photocurrents in any desired wavelength range from 2 to 30 μm. The schematic band alignment shown in Fig. 2 illustrates the spatial separation of excited electrons and holes in the respective InAs and GaSb QW layers. Thus the reason for the band gap in a type-II SL is not the same as in a bulk material, and in particular the band gap is not given by Eq. (3). Modeling the band structure and the thermal shifts of a type-II SL is far more complex than a bulk system and has to be done numerically.

The change of the band gap with temperature was experimentally measured by photoluminescence for a 2-μm-thick mid-wavelength infrared (MWIR) type-II sample with each period consisting of 11 monolayers (MLs) of GaSb, 7 MLs of InAs, one pure InSb interface, with the other interface being $Ga_{0.2}In_{0.8}Sb$. The sample was not intentionally doped.

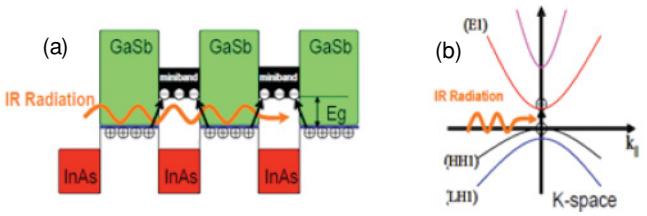

FIG. 2. (Color online) (a) Spatial band alignment in a type-II SL. Red stands for the InAs forbidden gap and green stands for the GaSb forbidden gap. The black regions are the electron and hole minibands. Hole minibands are much narrower, due to their large effective mass. (b) Schematic band structure with direct band gap and absorption process in K space.

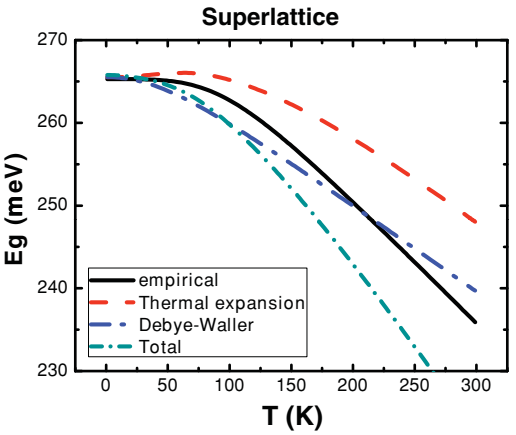

FIG. 3. (Color online) Comparison between theory and experiment for a type-II SL using the same parameters presented in Table I. The change in the band gap is clearly overestimated.

Figure 3 shows the comparison between the calculated shrinkage of the band gap in this material using the empirical TB model[22] with the same parameters that were developed for the bulk material (shown in Table I) and the empirical curve taken from experimental values.[33] The DW term and the expansion coefficient in the SL were assumed to be the same as the bulk material in each individual layer. Since all the materials are forced to have the same lattice constant in the parallel plane equal to the underlying GaSb substrate, their distance in the growth direction is adjusted based on their elastic constants. It is clear from Fig. 3 that using the same parametrization as the bulk material overestimates the change in the band gap. Also, the percentage of the total change due to the expansion and the DW term are approximately equal, which is in contradiction to the bulk material where it was ~40% and 60%, respectively. However, it should be noted that both the DW term and the expansion coefficient are determined by the phonon spectrum of the material, which is expected to be strongly modified in the SL compared to the bulk material. Therefore, it is not surprising that the same parameters that worked for the bulk material do not provide a good fit for the SL. In the following, it is assumed that a proper modification of the n values for the SL can properly account for all the modifications in the phonon spectrum.

To achieve a fit with the experiment for the SL, we need to reduce the n value for each material by ~20%. The unique n values that were used are shown in Table II. Figure 4 shows the result of the fitting. We note that the fitted curve gives good agreement above a critical temperature $T \sim 50$ K, but below it tends to overestimate the magnitude of the band gap (green dashed line). However, this overestimation is of the order of

TABLE II. Values of n in Eq. (6) that are chosen to fit the experimental data in the SL.

Material	n
GaAs	3
GaSb	2.8
InAs	2.4
InSb	2.4

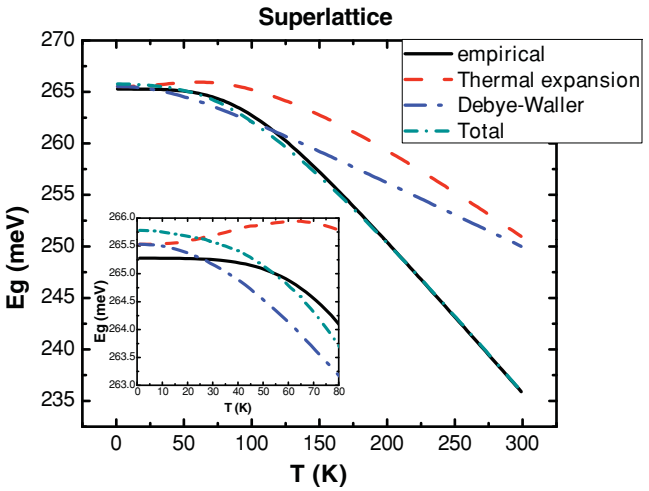

FIG. 4. (Color online) Comparison between theory and experiment for a SL using the parameters in Table II.

0.5 meV, as shown in the inset of Fig. 4, which is almost within the accuracy of the experimental method in determining the band gap. The slope of the expansion term at high temperature stays at 60% of the total slope while the DW term has a slope that is ∼40% of the total slope, exactly opposite to the bulk material case.

Figure 5 presents the actual SL band structure with the best parameters in the plane and growth (SL) directions for two different temperatures $T=0$ and $T=300$ K. In general, we find that temperature does not produce any unusual effects. It rigidly shifts the bands. The apparently anomalous curvature of the valence bands is a common occurrence in SLs and is due to band mixing (see, for example, Ref. 34).

V. CONCLUSION

A theory was developed to calculate the shrinkage of the band gap with temperature in semiconductors using a tight-binding method. In this method, it was decided to first define a disturbed lattice which still obeys Bloch's law via an effective lattice constant evaluated from the mean-squared displacement of the atoms from each other. The thermal displacement method favors the larger displacement in contrast to the thermal averaging of the overlaps. If the overlap energy is expanded using a Taylor series before taking the time average, the answer will be qualitatively different and the DW term will act in the opposite direction (increasing the band gap). This is the result that we would also get if we used perturbation theory to calculate the second-order term (DW) in the electron-phonon interaction. Once the unique structure and band structure are generated, we can compute thermal polaron shifts and the softening effect. The polaron effects for electron-phonon interaction were calculated, but the simple calculations showed that the total effect is less than 10% and it was neglected in fitting the experimental data. The softening term was dropped as well since it was not determined to be the dominant mechanism, and its ad hoc derivation could have easily overestimated the effect.

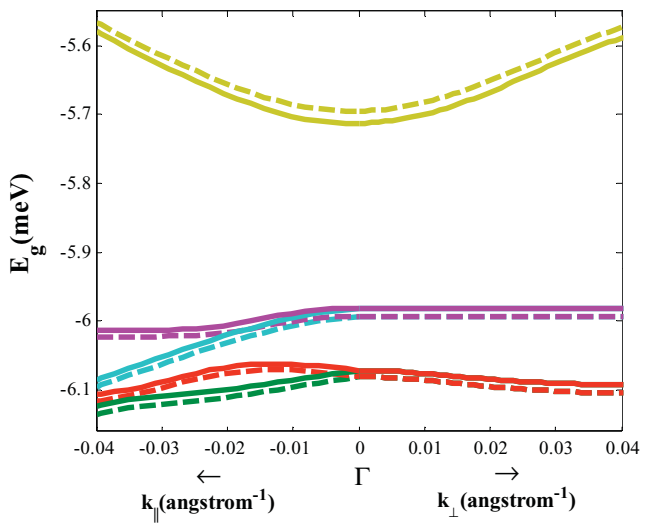

FIG. 5. (Color online) Type-II superlattice band structure calculated using the empirical TB method at 0 K (dashed lines) and 300 K (solid lines)

For fitting the experimental data, the power n in the overlap $1/d^n$ scaling rule was used as the fitting parameter to fit the experimental data. The values of n ranged from 2.9 for InAs to 3.7 for GaAs. The fact that the model was able to give close to perfect fits to the experimental data is an indication that the essential physics mechanism involved in the thermal energy shift are indeed the lattice expansion and the thermally induced fluctuations of the relative positions of the atoms in agreement with the work of Cody *et al.*[21] The thermal disorder causes the overall interatom coupling to be weakened while atoms are moving both in the harmonic and anharmonic parts of the potentials. In all the materials studied in this paper, after fitting the experimental data by choosing proper values for n, it was observed that the contribution due to expansion coefficient was ∼40% of the total change while the Debye-Waller term accounted for ∼60% of the total change.

The change of band gap with temperature in InAs/GaSb type-II SLs was also studied. Photoluminescence measurements, recently performed in our group, were used to determine the experimental change of the band gap with temperature and the theory that was developed for the bulk material was applied to explain the observations. Using the same parameters for the SL as for the bulk material, the band-gap change in the SL was overestimated. But by reducing the value of n by ∼20% for all materials, a proper fit for the SL was also achieved, despite the enormous complexity. The discrepancy between the fitting parameter of the bulk materials and the SL was mainly attributed to the modification of the phonon spectrum in the type-II SL, a result of the more complex structure. It was observed that the empirical rule observed in the bulk material was reversed for the SL, and the expansion and DW terms accounted for 60% and 40%, respectively, of the total change in the band gap.

ACKNOWLEDGMENT

The authors thank Stanley Tsao (Center for Quantum Devices, Northwestern University) for helpful discussions and comments on the manuscript.

[1]Y. P. Varshni, Physica **34**, 149 (1967).
[2]R. Pässler, Solid State Electron. **39**, 1311 (1996); J. Appl. Phys. **82**, 2611 (1997); **83**, 3356 (1998); **88**, 2570 (2000); **89**, 6235 (2001); **101**, 093513 (2007).
[3]H. Y. Fan, Phys. Rev. **82**, 900 (1951).
[4]G. D. Mahan, J. Phys. Chem. Solids **26**, 751 (1965).
[5]P. B. Allen, Phys. Rev. B **18**, 5217 (1978).
[6]P. B. Allen and M. Cardona, Phys. Rev. B **27**, 4760 (1983).
[7]S. Chuang, *Physics of Optoelectronic Devices* (Wiley, New York, 1995), p. 124.
[8]R. Passler, J. Appl. Phys. **101**, 093513 (2007).
[9]K. P. O'Donnell and X. Chen, Appl. Phys. Lett. **58**, 2924 (1991).
[10]D. Olguín, A. Cantarero, and M. Cardona, Phys. Status Solidi B **220**, 33 (2000).
[11]V. Heine and J. A. Van Vechten, Phys. Rev. B **13**, 1622 (1976).
[12]B. Ridley, *Quantum Processes in Semiconductors* (Clarendon, Oxford, UK, 1999), p. 37.
[13]Y. Wei, Ph.D. thesis, Northwestern University, 2005.
[14]Y. Wei and M. Razeghi, Phys. Rev. B **69**, 085316 (2004).
[15]W. A. Harrison, Phys. Rev. B **24**, 5835 (1981).
[16]P. Vogl, H. P. Hjalmarson, and J. D. Dow, J. Phys. Chem. Solids **44**, 365 (1983).
[17]C. Priester, G. Allan, and M. Lannoo, Phys. Rev. B **37**, 8519 (1988).
[18]C. Priester, G. Allan, and M. Lannoo, Phys. Rev. B **38**, 13451 (1988).
[19]S. Krishnamurthy, A. Chen, A. Sher, and M. Van Schilfgaarde, J. Electron. Mater. **24**, 1121 (1995).
[20]J. Ziman, *Principles of the Theory of Solids* (Cambridge University Press, Cambridge, UK, 1979), p. 62.
[21]G. D. Cody, T. Tiedje, B. Abeles, B. Brooks, and Y. Goldstein, Phys. Rev. Lett. **47**, 1480 (1981).
[22]Y. Wei and M. Razeghi, Phys. Rev. B **69**, 085316 (2004).
[23]A. Blacha, H. Presting, and M. Cardona, Phys. Status Solidi B **126**, 11 (1984).
[24]E. Grilli, M. Guzzi, R. Zamboni, and L. Pavesi, Phys. Rev. B **45**, 1638 (1992).
[25]O. Madelung, *Introduction to Solid-State Theory* (Springer, Berlin, 1996), p. 186.
[26]N. Miura, H. Nojiri, P. Pfeffer, and W. Zawadzki, Phys. Rev. B **55**, 13598 (1997).
[27]P. W. Anderson, Nature (London), Phys. Sci. **235**, 163 (1972).
[28]M. Cardona, T. A. Meyer, and M. L. W. Thewalt, Phys. Rev. Lett. **92**, 196403 (2004).
[29]C. Ghezzi, R. Magnanini, A. Parisini, B. Rotelli, L. Tarricone, A. Bosacchi, and S. Franchi, Phys. Rev. B **52**, 1463 (1995).
[30]Z. M. Fang, K. Y. Ma, D. H. Jaw, R. M. Cohen, and G. B. Stringfellow, J. Appl. Phys. **67**, 7034 (1990).
[31]R. Pässler, J. Appl. Phys. **89**, 6235 (2001).
[32]S. Adachi, *Handbook on Physical Properties of Semiconductors* (Springer, Berlin, 2004).
[33]D. Hoffman, Ph.D. thesis, Northwestern University, 2009.
[34]E. Rosencher and B. Vinter, *Optoelectronics* (Cambridge University Press, Cambridge, UK, 2002), p. 394